

(2)

AD-A153 759

NRL Memorandum Report 5529

Infrared Halo Effects Around Ships

I. B. SCHWARTZ, K. A. SNAIL, AND J. R. SCHOTT

*Advanced Concepts Branch
Optical Sciences Division*

March 29, 1985



2 DTIC
SELECTED
MAY 15 1985
S D
B

NAVAL RESEARCH LABORATORY
Washington, D.C.

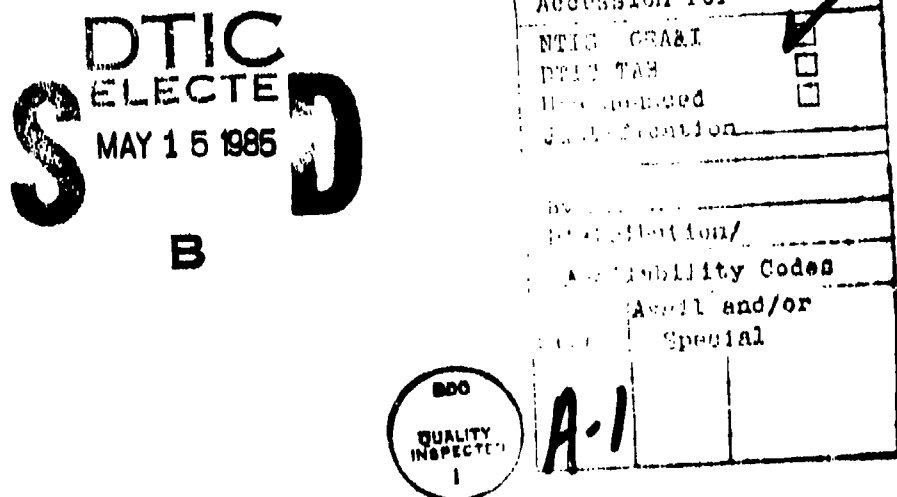
Approved for public release; distribution unlimited.

REPORT DOCUMENTATION PAGE

1a. REPORT SECURITY CLASSIFICATION UNCLASSIFIED		1b. RESTRICTIVE MARKINGS	
2a. SECURITY CLASSIFICATION AUTHORITY		3. DISTRIBUTION/AVAILABILITY OF REPORT	
2b. DECLASSIFICATION/DOWNGRADING SCHEDULE		Approved for public release; distribution unlimited.	
4. PERFORMING ORGANIZATION REPORT NUMBER(S) NRL Memorandum Report 5529		5. MONITORING ORGANIZATION REPORT NUMBER(S)	
6a. NAME OF PERFORMING ORGANIZATION Naval Research Laboratory	6b. OFFICE SYMBOL <i>(If applicable)</i> Code 6520	7a. NAME OF MONITORING ORGANIZATION Office of Naval Research	
6c. ADDRESS (City, State, and ZIP Code) Washington, DC 20376-5000		7b. ADDRESS (City, State, and ZIP Code) Arlington, VA 22217	
8a. NAME OF FUNDING/SPONSORING ORGANIZATION Office of Naval Research	8b. OFFICE SYMBOL <i>(If applicable)</i>	9. PROCUREMENT INSTRUMENT IDENTIFICATION NUMBER	
8c. ADDRESS (City, State, and ZIP Code) Arlington, VA 22217		10. SOURCE OF FUNDING NUMBERS	
PROGRAM ELEMENT NO. 61153N	PROJECT NO.	TASK NO.	WORK UNIT ACCESSION NO. DN380-425
11. TITLE (Include Security Classification) Infrared Halo Effects Around Ships			
12. PERSONAL AUTHOR(S) Schwartz, I.B., Snall, K.A., and Schott, J.R.			
13a. TYPE OF REPORT Interim	13b. TIME COVERED FROM 9/83 TO 9/84	14. DATE OF REPORT (Year, Month, Day) 1985 March 29	15. PAGE COUNT 16
16. SUPPLEMENTARY NOTATION			
17. COSATI CODES		18. SUBJECT TERMS (Continue on reverse if necessary and identify by block number) Infrared Ship signatures	
FIELD	GROUP	SUB-GROUP	
19. ABSTRACT (Continue on reverse if necessary and identify by block number) Accurate infrared ship signature codes are needed by the Navy in order to predict signatures of existing ships, test algorithms used for detection, classification and homing, study signature reduction techniques, and reduce the IR detectability of future vessels. Currently, the signature codes being used by the Navy do not include contributions from radiation undergoing one or more reflections off surfaces between the ship and sensor. In most instances, reflected infrared radiation can be neglected since the absorptance of most reflecting surfaces (e.g. water, painted surfaces, etc.) is high in the infrared. However, for the case of grazing or near-grazing incidence on a water surface, the IR reflectivity becomes very large. Hence, low angle observations of the sea near a ship tends to show a warmer region in front of the ship; in rough seas the IR image of the ship's reflection is blurred into an infrared "halo". Recent infrared field measurements performed by NRL on the USS Ticonderoga clearly show the halo effect. In this report we determine the mean temperature difference between the halo and background for a Ticonderoga image, and then propose a simple one-dimensional model for the angular dependence of the halo's apparent temperature.			
20. DISTRIBUTION/AVAILABILITY OF ABSTRACT <input checked="" type="checkbox"/> UNCLASSIFIED/UNLIMITED <input type="checkbox"/> SAME AS RPT <input type="checkbox"/> DTIC USERS		21. ABSTRACT SECURITY CLASSIFICATION UNCLASSIFIED	
22a. NAME OF RESPONSIBLE INDIVIDUAL I. B. Schwartz		22b. TELEPHONE (Include Area Code) (202) 767-2045	22c. OFFICE SYMBOL Code 6520

CONTENTS

INTRODUCTION	1
DATA ANALYSIS: MOTIVATION FOR A HALO MODEL	1
THEORY: ONE DIMENSIONAL MODEL OF INFRARED HALOS	2
Non-Haloed Sea Signature	3
Halo Signature	3
Halo-Sea Contrast	3
Ship-Halo Contrast	4
CONCLUSIONS	4
ACKNOWLEDGMENTS	5
REFERENCES	15



INFRARED HALO EFFECTS AROUND SHIPS

INTRODUCTION

Since the advent of infrared FLIR's, the Navy has made a significant commitment to modelling the infrared signature of Navy vessels. In addition, many infrared measurements of ships in a sea background have been made in order to determine the contrast between a target (ship) and its background. Since measurements are expensive, modelling is usually considered as a viable economic alternative. In order to simulate the signature of a ship in various environmental settings, it is necessary to model the entire scene accurately. This paper considers the ship-sea interface and its effect upon the signature of the scene.

Over the last few years, the Navy has been using two ship signature codes known as SIRS¹ and SIREOS², and a third (SSIRM) has been under development at NRL³. The SIREOS code is essentially an embellishment of the SIRS code, but neither code considers the reflection of the ship's thermal emissions off the sea surface. The fact that ship-water reflections contribute significantly to the infrared signature of a ship has been observed qualitatively in ship infrared imagery⁴. In this report a more quantitative approach will be applied to imagery of the U.S.S. Ticonderoga⁵, confirming the conclusion that infrared 'halos' make a significant contribution to ship IR signatures.

The purpose of this paper is thus two-fold. First, we motivate the modelling of the ship-sea interface by examining imagery of the Ticonderoga in the longwave infrared band. It is shown that the geometry of the scene has a measurable effect upon the radiometry of the signature. In the second part of this report we use a one-dimensional model to examine the radiance of reflections of the ship off the water to a given point in space. The effect of the emissivity's angular dependence on the radiance is included, and the total radiance as a function of view angle is computed.

DATA ANALYSIS: MOTIVATION FOR A HALO MODEL

During the previous year, NRL's Advanced Concepts Branch has performed extensive infrared measurements of the U.S.S. Ticonderoga at sea. These measurements were made with an Inframetrics model 210 dual-band sensor with a NEAT of .1 deg C and a resolution of 2 mr in the LWIR band (8-12 μ m). Figure 1a and 1b are examples of Ticonderoga images in the 8-12 μ m band. Both of these images have been contrast stretched to enhance the image and to bring out the relevant features for our discussion.

Manuscript approved December 14, 1984.

In both the upper and lower images, one can see an apparently warmer region of the sea just below the ship which is caused by reflected thermal radiation off the water; this 'halo' effect is most pronounced near the bow of the ship. In both images, one sees a "V"-shape near the bow which locates the water line of the ship. In addition, the spatial spread of the halo extends out more than the height of the hull due to reflections of thermal radiation from the superstructure and exhaust stacks. The result is a ship in a brightened background, hence the term 'infrared halo'.

One can get an estimate of how much the halo contributes to the overall radiance of the scene by enclosing the halo with a boundary and then computing the mean temperature within that boundary. The same boundary outline can then be translated to a region of the sea where negligible ship radiation is reflected to the sensor and the mean temperature can be computed as before. For the halo pictured in Fig. 2, the region enclosed in the red boundary was found to have a mean blackbody temperature of 293.2 ± 0.3 degrees Kelvin. The background region enclosed within the green boundary has a mean temperature of approximately 292.3 ± 0.3 degrees. Contrasting the temperature of the halo with its background yields a mean temperature difference of $.9 \pm .5$ degrees, which can be an order of magnitude above the sensitivity of most present day FLIR's.

Although only one set of data has been analyzed here, we have also observed that as the viewing angle (as measured from the normal to the sea surface) increases, the size and extent of the halo also increases. An analysis of the spatial extent of the halo is not considered here, but is treated in a future report.

THEORY: ONE DIMENSIONAL MODEL OF INFRARED HALOS

We wish to point out that an infrared halo around a ship can be understood in terms of a simple one dimensional model of the radiative transfer between the ship, sea surface and sensor. In this model, the in-band ($8-12 \mu\text{m}$) radiation leaving the sea surface in the vicinity of a ship consists of two components: emissions from the water and emissions from the ship that are reflected off the water (see Figure 3). As the viewing angle, θ , increases beyond 60 degrees, the reflectance of the sea surface increases rapidly, causing the observed temperature increase of the sea. For calm sea states and near grazing observation angles we expect to see a mirror image of the ship's thermal signature below the water line.

The following assumptions were made in modelling the infrared halo of a ship:

- (1) The sea surface is smooth, that is, the wind speed is zero.
- (2) The ship can be approximated by a vertical plate.
- (3) The ship surfaces have a Lambertian gray-body emittance of 0.9.
- (4) The sensor spectral response is one for $8.0 < \lambda < 12.0 \mu\text{m}$ and zero otherwise.

Non-Haloed Sea Signature

Under the above assumptions, the radiance reaching the sensor's aperture which appears to originate from a non-halo area of the sea, L_n , is represented by the sum of the radiance of the water, L_w , the sensor-sea path radiance, L_p , and the reflected sky radiance, L_r . Letting $\tau(\lambda)$ denote the transmittance of the atmospheric path from the plate to the sensor and $\epsilon(\lambda, \theta)$ the emittance of the sea water, we can write the radiance from the non-haloed sea as

$$L_n(\theta) = \int_8^{12} L_p(\lambda) d\lambda + \int_8^{12} \tau(\lambda) \epsilon(\lambda, \theta) L_w(T_w) d\lambda + \int_8^{12} \tau(\lambda) [1 - \epsilon(\lambda, \theta)] L_r d\lambda \quad (1)$$

where T_w is the temperature of the sea. Notice that no averaged quantities are used in this model, rather, the terms in Eq. (1) are integrated over the 8-12 band. The transmittance, $\tau(\lambda)$, is computed using LOWTRAN 5, modified to calculate path radiances using a technique suggested by Shalom. The emissivity of water, $\epsilon(\lambda, \theta)$, is calculated from the real and imaginary parts of the index of refraction of water using Fresnel's equations for absorbing media. The blackbody spectral radiance of the water and ship were calculated from Planck's law:

$$L_w(T_w) = 2.0 c_1 / \lambda^3 [\exp(c_2/\lambda T) - 1] \quad (2)$$

where:

$$\begin{aligned} c_1 &= 5.9547 \times 10^{-8} \text{ Watts (micron)}^3/\text{sr} \\ c_2 &= 1.4388 \times 10^4 \text{ micron K} \end{aligned}$$

Halo Signature

The total in-band radiance reaching the sensor's aperture from haloed portions of the sea can be written as:

$$L_H = \int_8^{12} L_p(\lambda) d\lambda + \int_8^{12} \tau(\lambda) [\epsilon_s(\lambda, \theta) L_w + \epsilon_{sp}(\lambda, \theta) L_s] d\lambda \quad (3)$$

where:

$$\begin{aligned} \epsilon_s &= \text{average LWIR emittance of ship surfaces} \\ \epsilon(\lambda, \theta) &= \text{spectral directional reflectance of water} \end{aligned}$$

Since the viewing angles we are interested in are near grazing and the ship surfaces producing the halo are vertical, the emission angle for the paint is normally less than 60 degrees. Therefore, we expect the approximation of an angle independent ship emittance to be fairly accurate since the emittance of a typical paint is usually Lambertian out to about 60 degrees.

Halo-Sea Contrast

The contrast radiance between the halo and non-halo portions of the sea can be written as:

$$\Delta L = \int_8^{12} \tau(\lambda) \rho(\lambda, \theta) [\epsilon_s L_s - L_r] d\lambda \quad (4)$$

We have been primarily interested in cases where the sign of ΔL is positive. However, under certain circumstances the halo contrast radiance may go negative, that is, the ship radiance may be less than the sky radiance. For horizontal paths through the atmosphere, L_s is essentially equal to the radiance of a blackbody at the temperature of the atmosphere. As the elevation angle increases, the emissivity decreases rapidly in spectral regions where the atmospheric absorption is low. As an example, at 15 degrees up from the horizontal, the sky radiance at 10 μm is already reduced to less than 30% of the radiance of a blackbody at the air temperature of the lower atmosphere. Depending on the relative temperatures of the air and ship, the halo will be either positive or negative contrast with respect to the sea background. One situation under which the halo's contrast radiance might be negative would occur during or after a water washdown of the ship. If the water temperature is much less than the air temperature and if evaporative cooling effects are large enough, the ship surface temperatures may be reduced enough to cause a negative contrast halo.

In Figure 4 we show the angular dependences of the reflectance of water, averaged over the LWIR (8-12 μm) and MWIR (3-5 μm) bands. The in-band LWIR average transmittance of a U.S. standard atmosphere is shown as a function of viewing angle θ for a constant altitude sensor in Figure 5. Convolving these two effects and expressing the halo and sea radiances in terms of a blackbody equivalent temperature (see Appendix 1) allows one to calculate the apparent temperature increase of the halo for various sensor viewing angles. These results are shown in Figure 6. Note the rapid increase in temperature around 60 degrees due to the water's reflectance, and the subsequent decrease in temperature beyond 80 degrees due to the drop in atmospheric transmittance.

Ship-Halo Contrast

One can also examine the contrast between a ship and its halo. If we ignore radiation from the water which is reflected off the ship, we can write the ship-halo contrast radiance as:

$$\Delta L = \int_g^{12} [\epsilon_s L_s - \epsilon_w L_w - \epsilon_s L_s \rho_w] d\lambda \quad (5)$$

If we assume that the water surface is specular, then we can write Eq. (5) as:

$$\Delta L = \int_g^{12} \tau \epsilon_w(\theta) [\epsilon_s L_s - L_w] d\lambda \quad (6)$$

The sign of ΔL will depend on the relative temperatures of the ship and water, and the value of the ship's LWIR emittance. Paints typically have emittances of .90-.95 in the LWIR band. Major factors affecting the relevant temperatures include solar loading, air temperatures, internal heat sources, water washdown, etc.

CONCLUSIONS

In summary, two basic results have been presented in this paper. First, we have analyzed FLIR imagery in the 8-12 μm band and have

characterized a ship halo in a sea background. We observed from the image that the mean temperature increase of the halo was at least an order of magnitude greater than the sensitivity of present day sensors. Therefore, the halo is a measureable effect and should be accounted for in any imaging IR ship model.

Secondly, under several simplifying assumptions, we created a model to explain the apparent temperature increase of the sea due to the ship-sea interaction. It was observed that as a result of the angular dependence of the reflectivity of water, an infrared halo's radiance also varies with angle. Since the reflectivity of water increases with the viewing angle, the apparent temperature of the halo also increases. However, the atmospheric transmittance decreases rapidly for large angles and thus there is a maximum in the halo temperature around 70-80 degrees. Observations by a sensor near these angles of maximum contrast can be expected to show a large haloed area of the sea.

Since we have only considered a very simple model, there are many additional effects which need to be investigated. First, the spatial extent of the halo needs to be studied as a function of viewing angle and hull inclination angle. If one assumes a smooth sea surface, then it is easy to calculate the bounding lines of the halo. We have performed this calculation and our results will be presented in a future report. Second, what happens to the halo and its boundary when the sea is not smooth? Third, the halo temperature changes during ship washdowns should be quantified and modelled. Finally, one should also examine the effect of thin films and sea foam on the halo temperature, and polarization effects in the reflected radiation. In conclusion, the radiative transfer between a ship and the surrounding sea can make a significant contribution to the infrared signature of a ship and is an important research area for future IR ship models.

ACKNOWLEDGMENTS

The authors wish to thank Mr. Brent Lander for his assistance in analyzing the Ticonderoga imagery.



5:49:49PM
TUE MAR 29 83

COMPUTER ENHANCED

Fig. 1 — Long wave (8-12 μm) image of USS Ticonderoga



5:49:49PM
TUE MAR 29 83

ENHANCED IMAGE

3:20:32 AM
SUN FEB 28 83

Fig. 2 — Example of halo outlining routine

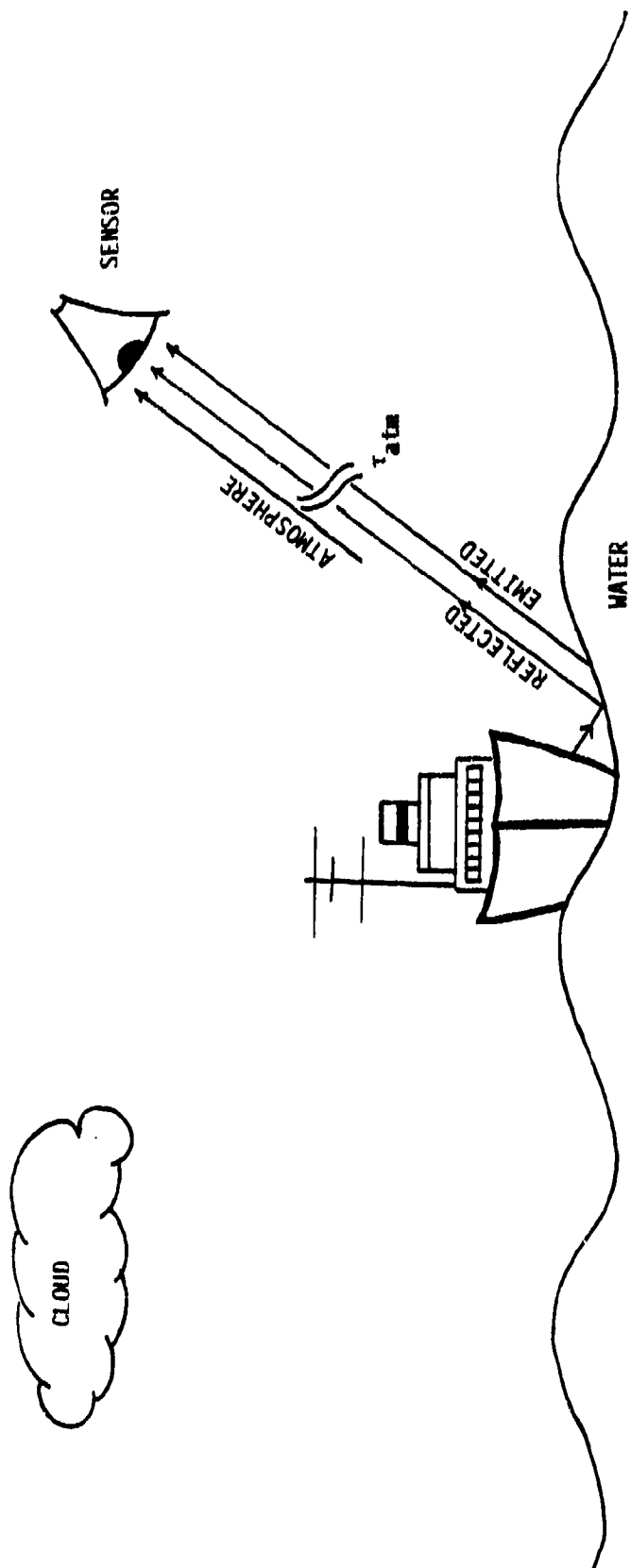


Fig. 3 — Schematic of contributions of halo signature

H₂O INFRARED REFLECTANCE VS. ANGLE

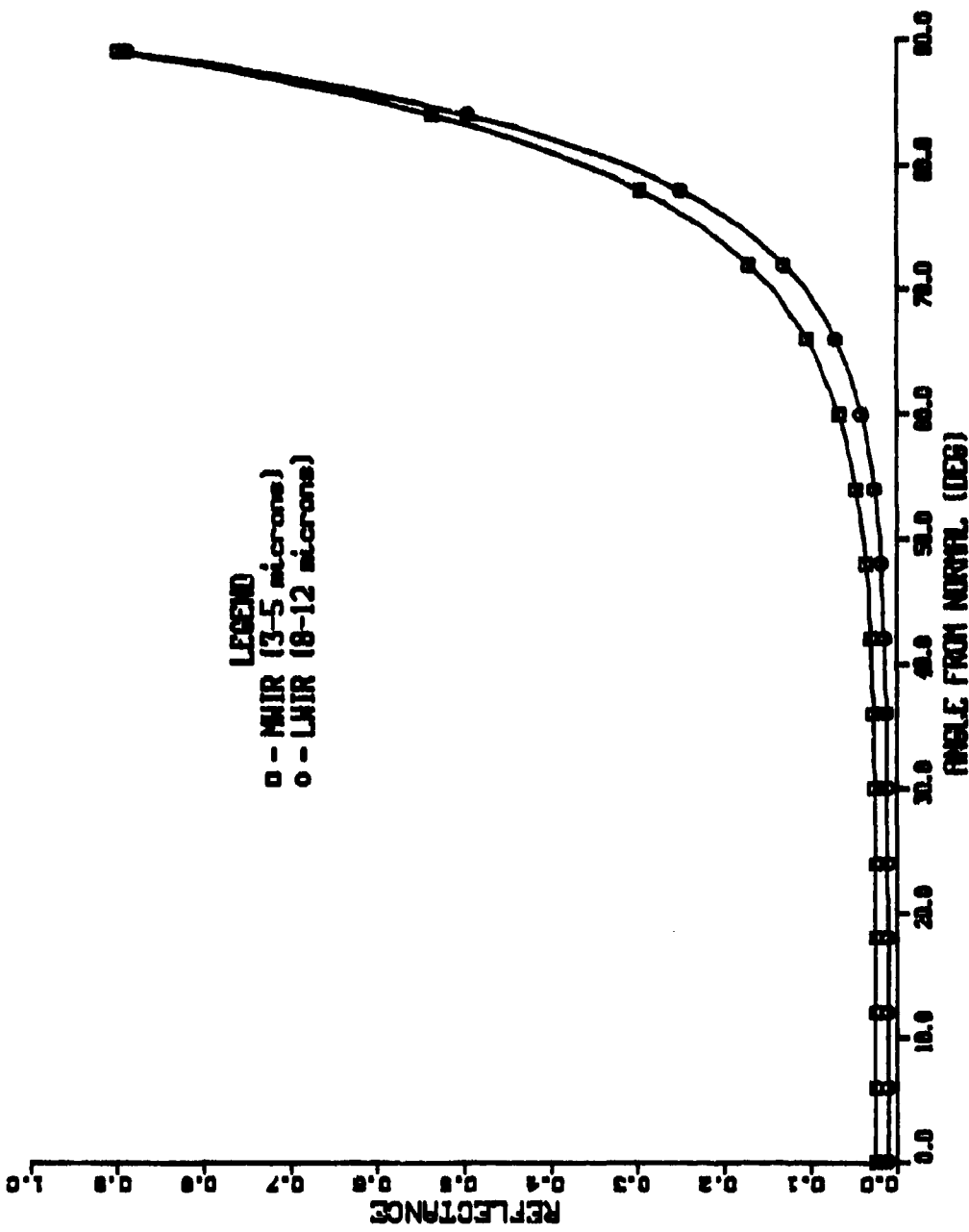


Fig. 4 — Angular dependence of water emissivity

LWIR ATMOSPHERIC TRANSMITTANCE VS. ANGLE

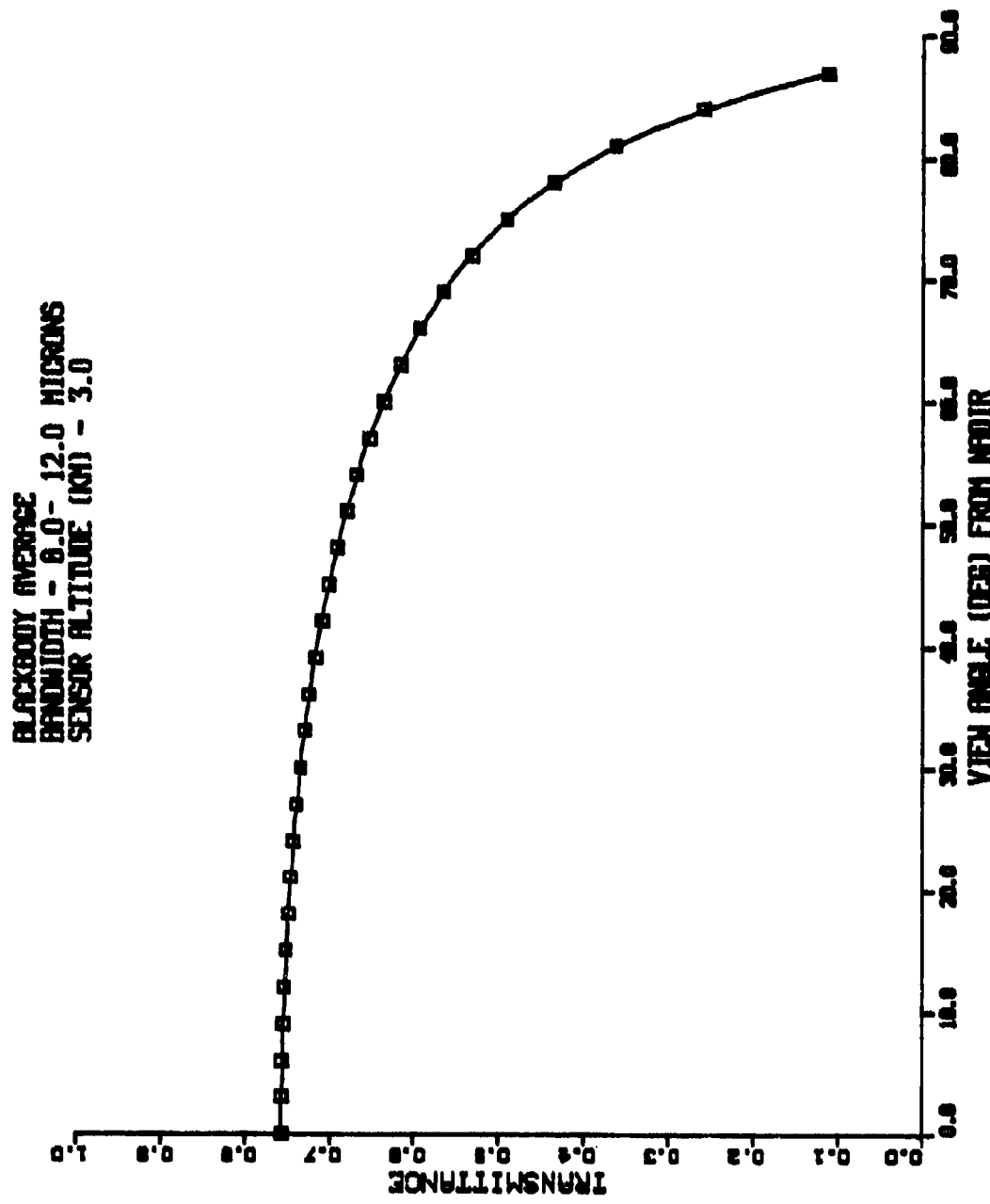


Fig. 5 — LWIR atmospheric transmittance of path between ship and constant altitude sensor

HALO TEMPERATURE INCREASE VS. ANGLE

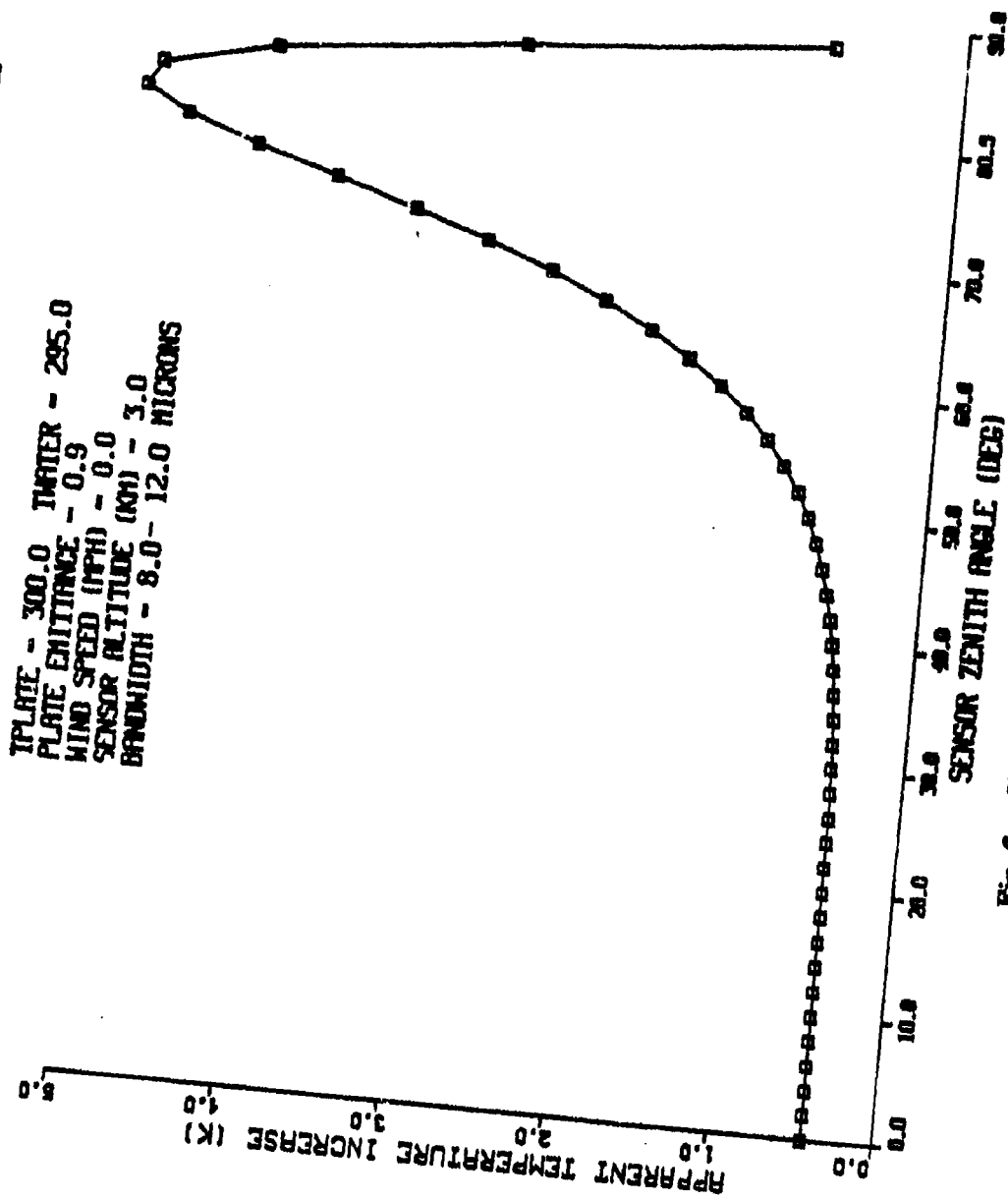


Fig. 6 - Halo temperature versus viewing angle

REFERENCES

1. Technical Overview and User's Manual, Reprint Number DTNSRDC-79/093, 1979.
2. Etherton, D.L., Initial Validation of the Ship Infrared Electro-Optical Scenario Computer Model, Report # DTNSRDC/C-SME-83/51, 1984.
3. T.G. Giallorenzi & J.M. McMahon, "A profile of NRL's Optical Sciences Division, part I. Laser and Sensor Development Programs", Laser Focus/Electro-Optics, May 1984, p. 74.
4. R.A. Eastley and W.H. Putnam, "Infrared Radiations from Naval Ships and Hydrofoil Patrol Gunboats (U): Quantitative analysis of low-angle measurements of ships and boats indicates high-radiance areas (U)", Naval Electronics Laboratory Center*, AD 512218, July 1970. See figures 2,17,18. *NELC-TR-1704
5. L. Massa, K. Whitney, and B. Lander, "Infrared Signatures of the CG47 USS Ticonderoga", NRL Report to be published
6. K.A. Snail, I.B. Schwartz, "Spatial Extent of Ship Infrared Halos", NRL Report, (to be published).
7. F.X. Kneizys, et. al., Atmospheric Transmittance/Radiance: Computer Code LOWTRAN 5, AFGL-TR-80-0067, Feb. 1980. AD-A088 215
8. A. Ben-Shalom, A.D. Devir, and S.Q. Lipson, Opt. Eng. 22, 460 (1983).
9. G. Yamamoto, M. Tanaka, and S. Asano, J. Atm. Sci. 27, 282 (1970).
10. E.M. Sparrow and R.D. Cess, Radiation Heat Transfer, Brooks/Cole, 1970.
11. R.D. Hudson, Infrared System Engineering, John Wiley & Sons, 1969, p. 108. AD-D501 193